Microsyst Technol (2017) 23:5677–5687
DOI 10.1007/s00542-017-3427-4

TECHNICAL PAPER

The design and analysis of a novel structural piezoresistive pressure sensor for low pressure measurement

Chuang Li[1,2] · Francisco Cordovilla[1] · José L. Ocaña[1]

Received: 26 January 2017 / Accepted: 27 April 2017 / Published online: 4 May 2017
© Springer-Verlag Berlin Heidelberg 2017

Abstract A micro electromechanical system piezoresistive pressure sensor with annularly grooved membrane combined with rood beam has been proposed for low pressure measurements based on silicon substrate. The model design, geometry analysis and performance prediction of the novel structure sensor are presented. Compared with other structural membranes, the proposed sensor achieves several advantages such as micro size, high sensitivity, low nonlinearity and stable dynamic behavior. Through analyzing the stress distribution of sensitive elements and the deflection of membrane by finite element method, the proposed structure can alleviate the contradiction between sensitivity and linearity to realize a device with high accuracy. The reasons why the proposed sensor can maximize sensitivity and minimize nonlinearity are also discussed. By localizing more strain energy in the high concentrated stress profile and creating partially stiffened membrane, the proposed sensor has achieved a high sensitivity of 34.5 mV/V/psi and a low nonlinearity of 0.25% FSS. Thus, the proposed structural sensor will be a better choice for low pressure applications less than 1 psi.

✉ Chuang Li
chuang.li01@alumnos.upm.es

[1] UPM Laser Center, Polytechnical University of Madrid, Carretera de Valencia, km. 7.3, 28031 Madrid, Spain

[2] Suzhou Changfeng Avionics Co., Ltd, 379, Jianlin Road, High-tech District, 215151 Suzhou, People's Republic of China

1 Introduction

Based on the transduction mechanisms of converting pressure input into electrical signal, pressure sensors are always classified as piezoresistive, capacitive, piezoelectric and resonant (Kumar and Pant 2014). Piezoresistive pressure sensors, due to their low cost, simple reading circuit, low energy consumption and mass producibility capability, have a wide range of applications leading to the highest amount of sales volume in the pressure sensor arena (Zhang et al. 2016). Especially for silicon piezoresistive pressure sensors, they constitute a large share in the micro electromechanical system (MEMS) mechanical sensor market (Li et al. 2016). The sensors utilize the silicon piezoresistive effect as the detection mechanism. Then a Wheatstone bridge is built up through electric connections with four P-type piezoresistors to transduce the resistance change into output voltage (Kumar and Pant 2015).

With the rapid development of micro/nano processing technology, recently, there is a strong demand trying to reduce the sizes of conventional sensors and enhance their sensitivity and linearity, namely getting a micro size sensor with high accuracy (Park et al. 2016). In certain case, sensitivity may be a more significant factor with not much constraint on linearity. For example, in case of a control switch which must indicate whether the pressure has reached a particular threshold value or not, linearity is not a critical factor. On the contrary, applications like level/altitude sensing using barometric sensors require a high degree of linearity (Kumar and Pant 2016). This is because severe nonlinearization will cause a high-sensitivity device of little practical value once nonlinearity is beyond a certain range (Rajavelu et al. 2014). Unfortunately, the trade-off between sensitivity and linearity is always irreconcilable for conventional pizoresistive pressure sensors, especially for low/

micro pressure measurement (Kumar et al. 2016; Yu and Huang 2015). The higher sensitivity is for the pressure measurement, the thinner membrane is for the sensor chip. However, a thinner membrane will cause a large membrane deflection which brings inferior linearity (Song et al. 2015). To alleviate the contradiction between sensitivity and linearity, previous efforts were mainly focused on (a) novel structures, (b) new materials and (c) compensation circuit.

a. The structure of piezoresistive pressure sensors always plays an important role in the performance. Design a novel structure with stress concentration regions (SCRs) and partially stiffened membrane (PSM) is an efficient way to improve sensitivity and linearity, simultaneously. To date, several new structural membranes, such as cross-beam membrane (CBM) (Tian et al. 2012), beam-membrane-mono-island (BMMI) (Yu et al. 2013), beam-membrane- dual-island (BMDI) (Meng and Zhao 2016), and beam-membrane-quad-island (BMQI) (Yu et al. 2015), all have achieved high sensitivity and linearity compared with the conventional structure sensors. The SCRs allow more strain energies to be utilized by piezoresistors, so the sensitivity can be improved definitely when resistors are placed on the SCRs (Sharma et al. 2013). Moreover, a low nonlinearity benefits from a small deflection because of the PSM, since the stiffness mutation restricts the deformation but not weakens the stress in the SCRs when the pressure is loaded on the surface of the membrane.
b. In order to improve the performance, many new raw materials for sensor chips were developed. For example, nanomaterials were not only adopted for the transistor design, but also applied as new sensing element or detection platform (Pramanik et al. 2006; Dau et al. 2013). Besides, some other novel materials, such as polysilicon (Wang and Li 2014), SiC (Fraga et al. 2010), diamond (Zhang et al. 2014b) and silicon nanowires (Zhang et al. 2014a) were all chosen to fabricate sensor chips to obtain high precision. Although the performance of those sensors has been improved by choosing these new materials, there are still some practical difficulties in mass production like immature technology, instable structure, unreasonable cost, etc.
c. To increase the accuracy of measurements, various kinds of compensation circuits and conditioning circuits were introduced to the packaging of sensors to improve the signal-to-noise ratio and measurement accuracy in practical applications of long-term transmission (Yao et al. 2016; Aryafar et al. 2015; Hao et al. 2014). However, this way not only adds the cost of the single device due to its complex fabrication process, but also lowers the overall reliability of the sensor, since a more complicated structure is easier to lose efficacy, so it can not fundamentally solve the contradiction between sensitivity and linearity. Besides, a complex circuit has to increase the cost of the device, which will lead to a decline in drastic market competitiveness (Li et al. 2014).

In consideration of above methods, it is found that design an integrated structure and finding out a balance between excellent sensing resolution and optimum linearity are the key concern (Mishra et al. 2015). As it is known, creating stress concentration regions, or even high concentrated stress profile (HCSP), are beneficial to gather the strain energy. The more strain energy concentration is, the higher sensitivity results. To solve the contradiction between sensitivity and linearity, a corrective measure is to locally stiffen the membrane thereby restricting partially the deformation, but not affecting the stress concentration. Moreover, the proposed structure should possess a smaller size compared with conventional C-type and E-type membrane structures. Then, the proposed sensor can satisfy the requirements of low pressure measurement for biomedical applications typically for body implanted with micro size (Alpuim et al. 2011).

This paper develops a novel structure annularly grooved membrane combined with rood beam to predict the electromechanical behavior of a piezoresistive pressure sensor under pressure of 1 psi (6.895 kPa). To reflect the advantages of the proposed structure, different membrane structures are modeled and compared by finite element method using COMSOL Multiphysics software to calculate the stress distribution, analyze the deflection of inherent structure and define the size of sensor. Based on the simulation results, the proposed structure can alleviate the contradiction between sensitivity and linearity to realize a device with high precision, micro size and stable machinery behavior. Therefore, the proposed structure sensor will be widely applied for low pressure applications.

2 Design and analysis

2.1 Design principle

The performance of sensors is determined by the maximum stress and linearity output. For the same membrane thickness, larger membranes offer high sensitivity with poor linearity and vice versa are true for smaller membranes. A square membrane, in pressure sensors, is chosen on account of its higher stress compared with rectangular and circular ones in the same conditions. On the basis of the theory of

elasticity, the maximum stress of the square, rectangular and circular membranes is given by the following equations (Hsu 2008):

$$\sigma_{sm} = 0.308P\left(\frac{L}{H}\right)^2(1-\mu^2) \tag{1}$$

$$\sigma_{rm} = 0.383P\left(\frac{B}{H}\right)^2(1-\mu^2) \tag{2}$$

$$\sigma_{cm} = 0.75P\left(\frac{R}{H}\right)^2(1-\mu^2), \tag{3}$$

where σ_{sm}, σ_{rm} and σ_{cm} are the maximum stresses for the square, rectangular and circular membranes, respectively. P the applied pressure; H the thickness of the membrane; μ the Poisson ratio; L the side length of the square membrane, B the width of the rectangular membrane, and R the radius of the circular membrane. By assuming that they have same membrane thickness H and identical applied pressure P, and that additionally, L is 1.2 times B and 2 times R, respectively, the following relationships can be obtained:

$$\sigma_{sm} = 1.16\sigma_{rm} = 1.64\sigma_{cm} \tag{4}$$

which means an ~15 and ~60% higher stress can be achieved by utilizing square membrane rather than the other two types.

There are two reasons for non-linearization of the pressure sensor, one is related to the excessive load on the membrane which directly destroys the linearity principle of the piezoresistive effect, and another is the oversized membrane deflection that changes linearity to nonlinearity in the relation between pressure and deformation. The case of excessive load on the membrane is not discussed in this work, after all, it belongs to an accident. Therefore, the case for oversized deflection will be the only discussed here. When the deflection exceeds the definite value compared to the thickness of membrane, the large deflection theories work, and then, the linearity relationship between deflection and pressure will change to nonlinearity. To resolve the problem of large deflection, a combination method developed by Foppl is adopted (Lin et al. 1999). This method combines small deflection theories on clamped boundary conditions and the membrane theories for large deflection problems on simply supported boundary conditions. Then, the total loading P is divided into two parts, namely, the bending stress and shearing stress represented by P_1 and membrane stress represented by P_2 ($P = P_1 + P_2$).

The loading P_1 is derived from the small deflection theory as:

$$P_1 = 71.3\frac{\omega EH^3}{L^4}. \tag{5}$$

The loading P_2 is derived from the large deflection theory as:

$$P_2 = 31.1\frac{\omega^3 EH}{L^4}. \tag{6}$$

These two equations are deduced separately and combined together in the end. For the large deflection, the equation can be shown as below:

$$\frac{PL^4}{EH^4} = 71.3\left(\frac{\omega}{H}\right) + 31.1\left(\frac{\omega}{H}\right)^3, \tag{7}$$

where PL^4/EH^4 is the relative load, ω/H is the deflection change relative to membrane thickness. By comparing the small and large deflection theories, the dimensionless deflection with respect to dimensionless load is presented in Fig. 1.

From the large deflection curve, it can be seen the relationship between the load and deflection is no longer linear when the relative deflection ω/H is exceeded 0.2. It indicates that the small deflection theory works only when the deflection is smaller than 1/5 thickness of membrane. Thus, the maximum deflection should be less than 1/5 thickness of the membrane, which is beneficial for obtaining low nonlinearity.

2.2 Structure design

A novel structure characterized by annularly grooved membrane with rood beam structure is proposed to measure low pressure less than 1 psi (6.895 kPa). N-type silicon wafer is chosen as the substrate of the sensor chip

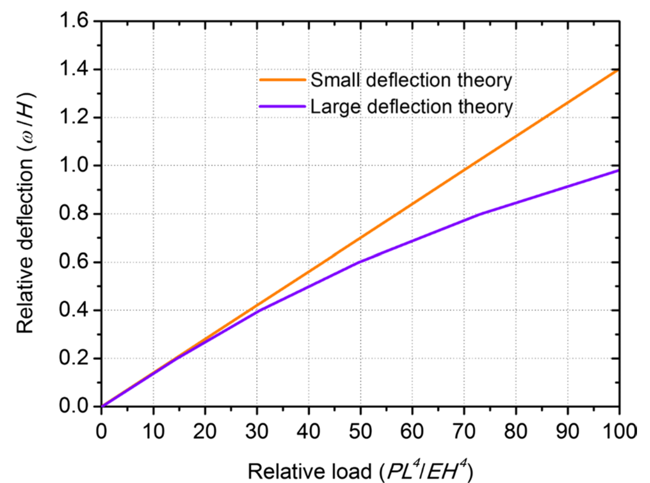

Fig. 1 Dimensionless deflection-load diagram for *square* membrane

owing to its desirable characteristics such as excellent mechanical properties and reproducible elastic deformations (Timoshenko and Woinowsky-Krieger 1959).

On the front side of the membrane, there are four grooves around the surface as shown in Fig. 2a. Moreover, four ribs are located between every two grooves which are just on the top of the gap between each beam and membrane edge. The membrane length and thickness are 3600 and 30 µm. The groove width and depth are 60 and 10 µm. A wheatstone bridge is built up through electric connections with the four piezoresistors on the surface of the rib regions.

On the rear side, a rood beam structure is placed as shown in Fig. 2b. The end of each rood beam is not connected with membrane edge, but remain at a 60 µm distance between them. The rood beam width is 200 µm and the thickness is 35 µm. An interesting phenomenon is that the rib length and width are equal to rood beam width and groove width respectively, which not only simplifies the fabrication processes, but also facilitates the dimensions optimization. By incorporating annular grooves and rood beam into the membrane, HCSP is expected to be formed to maximize the sensitivity; PSM is helpful for reducing the membrane deflection, and then minimize the nonlinearity.

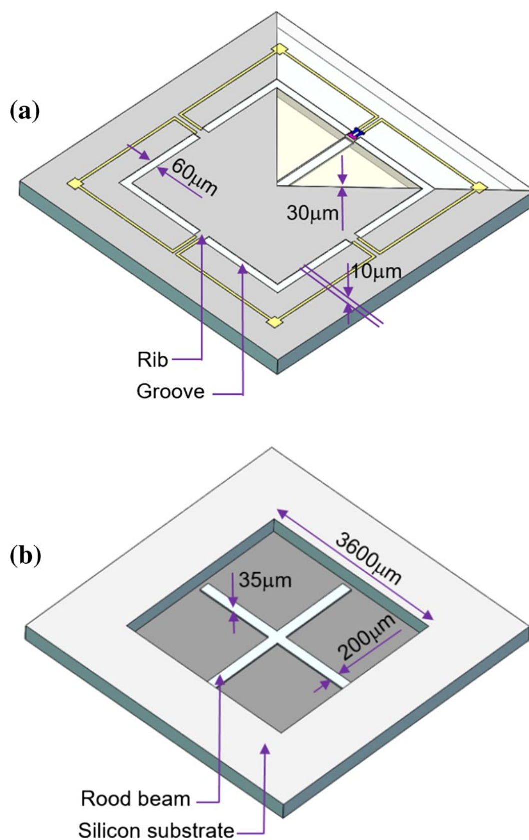

Fig. 2 Scheme of the proposed membrane. **a** Front side; **b** rear side

2.3 Geometry analysis

For the improved annularly grooved membrane combined with rood beam, it belongs to the EI-type sensor that is featured by grooved and bossed structure. Since the proposed structure with four grooves and bossed membrane presents a closed geometry with the EI-type, the central deflection ω can be expressed as followings (Yasukawa et al. 1989):

$$\omega = \frac{\pi L^2 b^3}{8bg^3 E(1+\beta)} P - \frac{3[1+\beta(g/H)^2]}{4(1+\beta)^2 g^2}\omega^3 \quad (8)$$

$$\beta = \frac{2gbE + g(\pi LE - 2bE)}{\pi LbD} \quad (9)$$

$$D = \frac{EH^3}{12(1-\mu^2)}, \quad (10)$$

where ω is the membrane deflection, β is the coefficient as defined by Eq. (9), D is the flexural rigidity, g and b are groove depth and width, L and H are membrane length and thickness, respectively. P is the applied pressure, E is the Young's elastic modulus, and μ is the Poisson ratio.

From the definition of the EI-type membrane deflection, ω can be treated as a subtraction of the rib bending strain [the 1st part of the Eq. (8)] minus the membrane deforming strain [the 2nd portion of Eq. (8)] (Yasukawa et al. 1989). It is noted that ω will be decreased by reducing the groove depth g and groove width b. In another word, the linearity can be improved by reducing the volume of the annular groove. According to previous studies, several theories should be considered: the membrane deformation should be under 1/5 membrane thickness based on small deformation theory discussed above; a plate is called "thin" when its ratio of thickness to the smaller span length is less than 1/20 (Ugural 1981); the thickness is usually above 10 µm for a good linearity according to the literature (Albert Chiou and Chen 2008), especially for those with the central bossed structure (Marco et al. 1996). If all factors are taken into consideration, the groove depth should be as close as possible to half of central membrane (Bao et al. 1991).

Additionally, one of initial conditions in the equations of bossed structure assumes a negligible bending moment at the central bossed-region under a certain pressure. Thus, the stiffness at the membrane center has to be much higher than that of the groove region because of the different thickness of the plate. Then, this stiffness mutation promotes the appearance of the HCSP at the rib region, which makes it possible to achieve high sensitivity. Since the thickness of the membrane edge is thinner than the center, there will be some losses in terms of stress. However, the introduction of the rood beam at the rear side of the membrane not only can compensate these losses, but also plays a role in partially

stiffening the membrane. Thus, the proposed structure is hopeful to alleviate the contradiction between sensitivity and nonlinearity and achieve a high performance.

3 FEM analysis

The performance of the proposed sensor chip is calculated by non-linear static analysis and modal analysis using the commercially-available finite element method (FEM) software COMSOL Multiphysics. The parameters of the single crystal silicon are as follows: Young's elastic modulus is 1.66×10^{11} N/m^2, Poisson ratio is 0.28. Figure 3 is the parameters setting of the FEM analysis. A fixed boundary conditions applied at the bonding site between the chip and the glass, and the nominal scale of the designed pressure sensor is set at 1 psi (6.895 kPa). In order to make the simulation results more accurate, there are 19,925 elements in the finite element module.

A typical membrane size of 3600 μm × 3600 μm and thickness of 30 μm are chosen for this study. Figure 4 depicts the von-Mises stress distribution and membrane deflection of the sensor chip at full scale pressure of 1 psi (6.895 kPa). The diagrams show that the maximum von-Mises stress is concentrated at the rib area and the maximum deflection is happened at the center of the membrane. In accordance with the previous discussion, the stress is mainly concentrated at the hinge area which is located at the rib surface, as indicated by the red area what is called the HCSP. This kind of high stress concentration profile just benefits from the unique structure for the membrane.

For the P-type [110] oriented silicon, the output (and therefore the sensitivity) of the sensor is proportional to the differential stress at the piezoresistor location and can be deduced by the approximate expression (Hsu 2008):

$$U_{out} = \frac{1}{2}\pi_{44}(\sigma_x - \sigma_y)U_{in} = \frac{1}{2}\pi_{44}\Delta\sigma_R U_{in}, \tag{11}$$

where π_{44} is the shear piezoresistive coefficient, σ_x is the transversal stress and σ_y is the longitudinal stress. Thus it can be seen that the differential stress $\Delta\sigma_R$ is an important indicator of the output voltage of the sensor. By the simulation results, the differential stress along x direction is shown in Fig. 5. The study region is closed to membrane edge and extend 100 μm inside and outside of this edge. The differential stress ($\sigma_x - \sigma_y$) are positively indicating that the maximum stress is located at a distance of 35 μm inside the membrane edge. Besides, it can be observed that the stress are mainly focused within a relatively small range (±100 μm), which means the strain energy is strictly limited in a narrow area on the surface of the rib region and the energy is not spread easily outside the HCSP. If the longitudinal piezoresistors are placed lengthwise along x direction

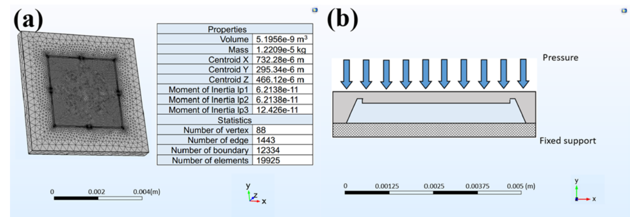

Fig. 3 Parameter setting of the FEM analysis. **a** Setting of mesh generation; **b** diagram of the fixed boundary condition and load

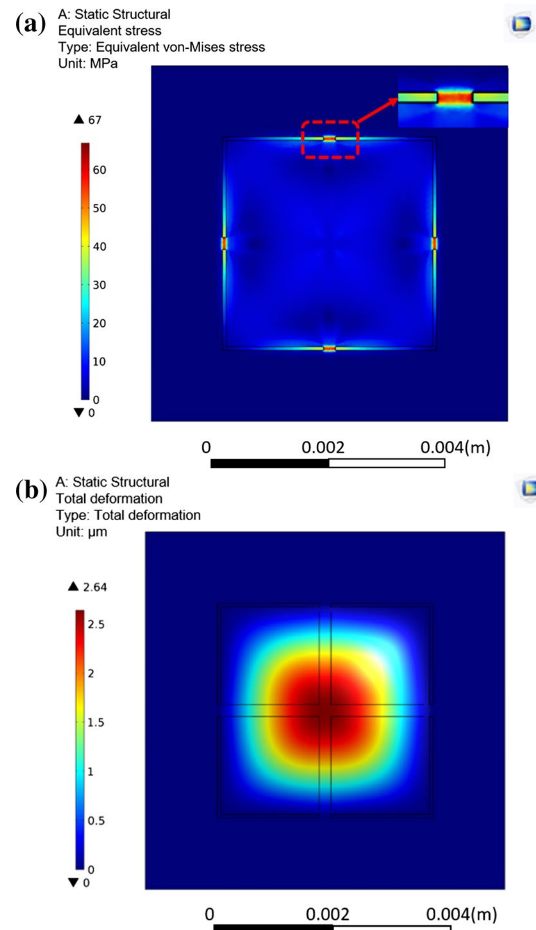

Fig. 4 Simulation results of the proposed membrane. **a** The stress distribution; **b** the deflection

and the transversal piezoresistors are placed breadthwise along y direction, the strain energy utilized by four piezoresistors will reach a maximum, which makes it possible to obtain even higher sensitivity.

The material properties of the silicon, aluminum and heavy doped silicon (piezoresistors) are listed in Table 1. Figure 6 shows the electric potential distribution and current density of the piezoresistors and wires with a 5 V power supply on the Wheatstone bridge. The output voltage

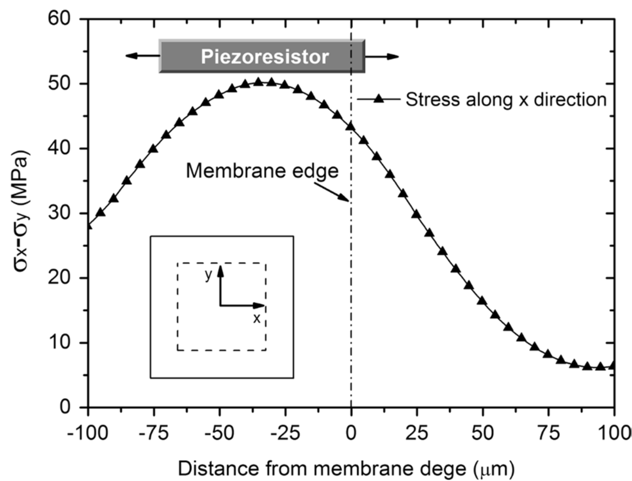

Fig. 5 Differential stress along x direction for the proposed membrane

of the proposed sensor is 2.5326 V minus 2.3701 V as shown in Fig. 6a, the output and sensitivity are equal to 172.5 mV and 34.5 mV/V/psi, respectively. In addition, a terminal current of 0.21 A is obtained as presented in Fig. 6b. The current flow "spreading out" into the sense electrodes (resistor place), this phenomena is defined as the "short circuit" effect (Bao 2005). The asymmetry in the potential, which is induced by the silicon piezoresistive effect, is also apparent in this figure.

4 Result and discussion

4.1 Membrane size

To prove the proposed structure can achieve a smaller size, the mechanical performance comparisons among proposed membrane, C- type and E-type membranes are studied under 1 psi uniform pressure, include maximum transversal stress and deflection by COMSOL. The three structures have the same membrane length and thickness as shown in Fig. 7a. Compared with the other two structures, the proposed structure has the highest stress and an intermediate deflection.

When the three membranes length and thickness are all set as the same dimensions, the C-type structure gets the lowest stress, which means a small output (or sensitivity) for C-type. To obtain high stress, an efficient method is to increase the ration of membrane length/membrane thickness. For example, the membrane length of C-type has to be 5776 μm, the stress can reach 65.1 MPa that is close to the proposed structure (see Fig. 7b), but the deflection will sharply increase to 15.7 μm which has exceeded 1/5 thickness of the membrane and not fit the small deflection principle anymore.

A kind of E-type structure pressure sensor is designed to decrease the large deflection of the C-type caused. As shown in Fig. 7c, the deflection is reduced to 1.84 μm by the introduction of the central mass. It can be concluded that the deflection of the E-type is smaller than C-type but the stress is also declined because of the hard core. It means the E-type has to sacrifice sensitivity when a low nonlinearity is achieved. If the maximum stress of E-type reaches the level of the proposed membrane, the membrane length should be at least 6752 μm. Then, the deflection for the E-type structure is 3.6 μm, which will lead to a worse linearity than the proposed membrane.

According to the above analysis, the proposed membrane possesses the advantage in size. The size of the sensor is decided by the membrane length and depth of the cavity. No matter for C- or E-type, the membrane is formed by chemical etching with 54.7° inclined walls, moreover, the etching cavity process is executed on one side of the silicon wafer (Hsu 2008). From Table 2, all the membranes are under 1 psi pressure. Cavity represents the etching depth, thickness is the membrane thickness and stress is the maximum transversal stress simulated by COMSOL. The table indicates, for example, when the membrane thickness is 30 μm, to achieve 65.1 MPa maximum stress, the membrane length of C- or E-type structures need almost 1.8 times the proposed structure, but the proposed structure just needs 3600 μm. It means that the proposed structure only requires approximate half size of the C- or E-type membranes for gaining the same stress.

4.2 Static performance

The static performance of the annularly grooved membrane combined with rood beam is compared with that of CBM structure (Tian et al. 2010) and BMQI structure (Yu and Huang 2015) under 1 psi (6.895 kPa) load as shown in

Table 1 Parameters of the proposed membrane

Material	Young's modulus (GPa)	Resistivity (Ω·cm)	Density (g/cm^3)	Piezoresistive coefficient (10^{-11}/Pa)
Silicon	166	2.3	2.3	–
Al	74	4.8×10^{-5}	2.7	–
P-doped silicon	168	2.3	2.3	$\pi_{11} = 6.6$; $\pi_{12} = -1.1$; $\pi_{44} = 138.1$

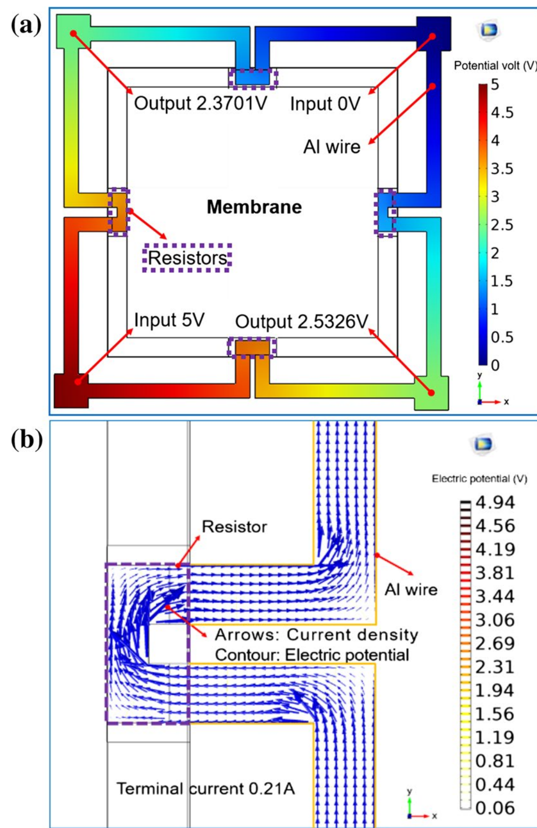

Fig. 6 Electromechanical behavior for the proposed sensor under 5 V power supply on the wheatstone bridge. **a** Electric potential; **b** current density

Fig. 8. The piezoresistive pressure sensors with CBM and BMQI structures also achieved a high accuracy to detect the low pressure. In this comparison, the materials, applied pressure and main dimensions of the three models are same. Compared with other two types, the sensitivity of the proposed structure reaches the largest value of 34.5 mV/V/psi (see Fig. 8d), which almost improves 36.2 and 22.5% compared with CBM and BMQI structures. The main reason is illustrated by the stress distribution shown in Fig. 8a. The stress of the proposed structure is concentrated in a smaller area than other two structures, even form a HCSP on the rib between every two grooves, so, the stress produced by the membrane deformation is also much bigger than other two types (see Fig. 8c). It indicates that the strain energy utilized by the resistors for the proposed structure is larger than others.

Based on the definition of the strain energy U, the U stored in the membrane under load can be expressed by Eq. (12) when the effective membrane area is substituted by the elementary area (Herrera-May et al. 2009):

$$U = \frac{D}{2} \iint_A \left(\frac{\partial^2 \omega}{\partial x^2} + \frac{\partial^2 \omega}{\partial y^2} \right)^2 dxdy - \iint_A \omega p(x, y) dxdy. \quad (12)$$

In Eq. (12), the potential energy U can be treated as a subtraction of the membrane bending strain [the 1st portion of the Eq. (12)] minus the surface load strain [the 2nd portion of Eq. (12)]. According to the small deformation theory, the transversal stress σ_x and longitudinal stress σ_y

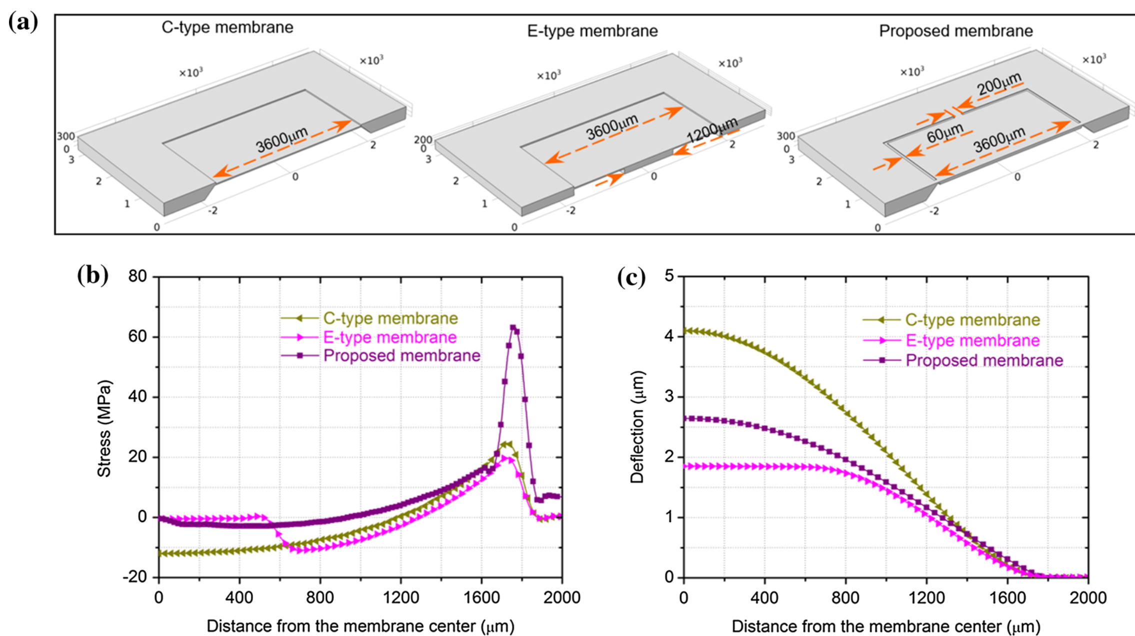

Fig. 7 Comparisons with C- and E-type structural membranes

Table 2 Comparison of structure size among various structures

Cavity (μm)	Thickness (μm)	Stress (MPa)	C length (μm)	E length (μm)	Proposed length (μm)
275	25	101.2	6028	7068	3600
270	30	65.1	5776	6752	3600
265	35	47.9	5525	6541	3600
260	40	41.8	5411	6322	3600

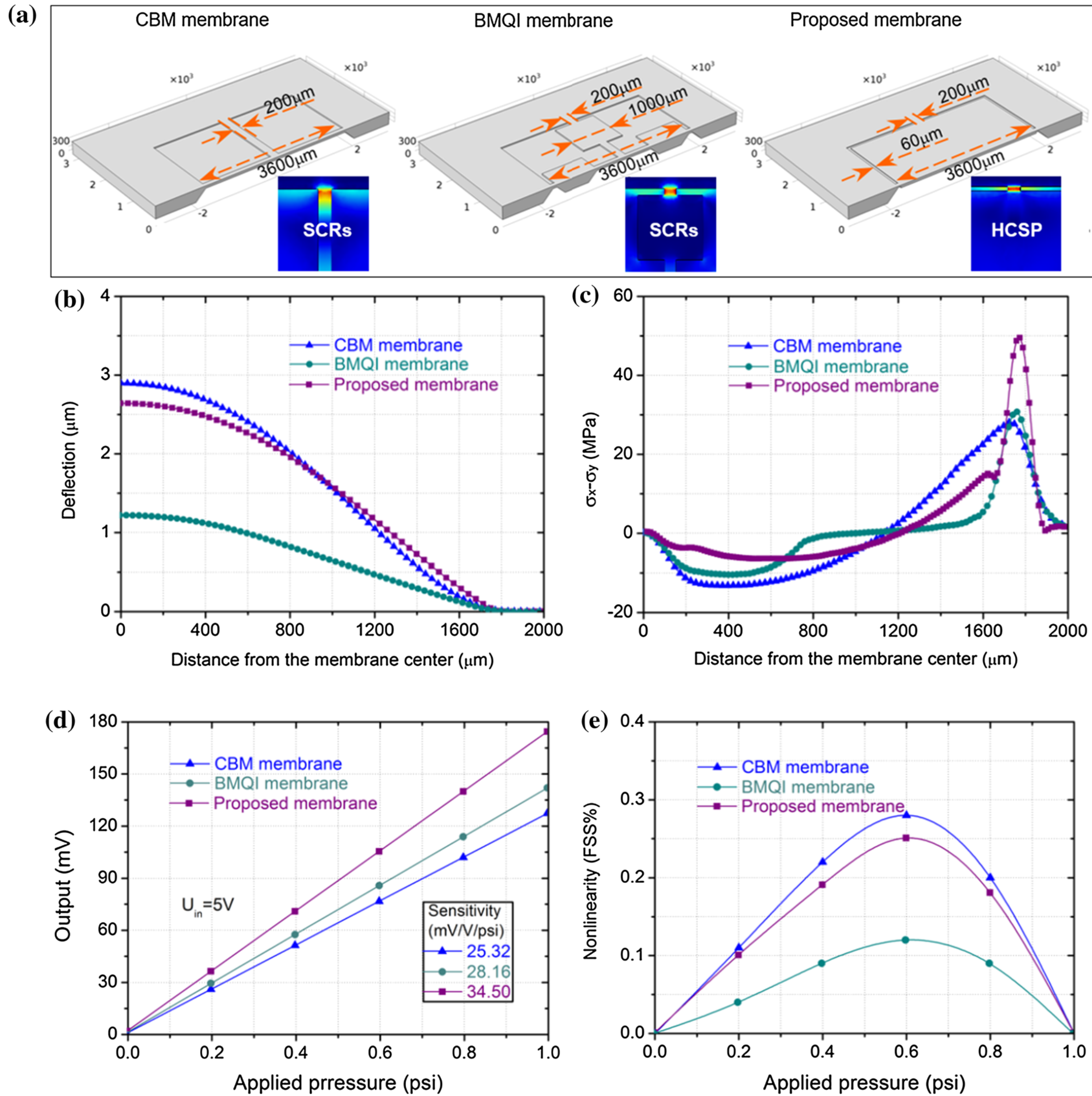

Fig. 8 Comparisons with the other two structural membranes

can be described as follows (Timoshenko and Woinowsky-Krieger 1959):

$$\sigma_x = -\frac{6D}{H^2}\left(\frac{\partial^2\omega}{\partial x^2} + \mu\frac{\partial^2\omega}{\partial y^2}\right) \tag{13}$$

$$\sigma_y = -\frac{6D}{H^2}\left(\frac{\partial^2\omega}{\partial y^2} + \mu\frac{\partial^2\omega}{\partial x^2}\right). \tag{14}$$

Introducing Eqs. (13) and (14) into Eq. (12) yields:

$$U = \frac{D}{2}\iint_A \frac{[2(\mu-1)(\sigma_x-\sigma_y)]}{Eh}dxdy - \iint_A \omega p(x,y)dxdy, \tag{15}$$

where H is the membrane thickness, A is the effective area of the membrane, and ω is the membrane deflection.

Through the comparison among different structures around the stress concentration region, the stress for the proposed membrane is much larger than other structures as seen in Fig. 8c. It also can be interpreted as the level of stress concentration for the proposed structure is higher than others as shown in Fig. 8a. In addition, the deflection for EI-type sensor is always smaller than traditional structures. Thus, the difference value between the 1st part and 2nd part of the Eq. (15) for the proposed sensor is relatively big.

In this improved membrane, the sensitivity is maximized by concentrating more strain energy at the position of the piezoresistors. This is successful achieved by two ways. On the one hand, the piezoresistors are placed on the narrow rib, which, due to its greater thickness than annular groove, provides a major portion of the support for the membrane. The function of the groove is to transfer more strain energy to the rib region, so the sensitivity will be improved. On the other hand, there is a gap between the rood beam and the membrane edge, which results in a stiffness mutation on the reverse side of the membrane. When the membrane experiences a deformation, the strain energy will reach to the gap place along the rood beam. With the piezoresistors near the highest stress surface of this rib, sensitivity is secondary to be enhanced. Thus, the proposed sensor can obtain the highest sensitivity compared with the other two structures.

From the Fig. 8e, it is noted that CBM, BMQI and proposed structures all achieve a low nonlinearity value less than 0.3%. Especially for the BMQI structure, it gets the lowest nonlinearity of 0.12% FSS. This is because the deflection for BMQI reaches the smallest value of 1.2 µm as presented in Fig. 8b. And yet, for the CBM, the nonlinearity is relative high due to the deflection almost reaching 3 µm. Non-linearization in the diaphragm-type piezoresistive pressure transducers happens when the diaphragm is deflected enough that it stretches. Then the geometry is deflected enough that the membrane starts to stretch in a non-linear manner and resists the applied pressure with membrane stress as in a balloon effect (Johnson et al. 1992).

In general, as the linearity improves, there is always some reduction in sensitivity. For the proposed membrane, the annular grooves are not only conducive to concentrate strain energy within a small area, but also create a greater deformation due to the stiffness change between the membrane center and edge. This is useful to obtain HCSP and then enhance the sensitivity, but, deteriorating linearity. However, the effect of rood beam on linearity assumes that it works like a strengthening rib. The rood beam reduces stretching of the rib at larger deflections, which in turn improves linearity. In contrast, the large open membrane area is relatively weak and free to stretch with minimum impact on linearity. Therefore, the conflict between high sensitivity and low nonlinearity is resolved by introducing annular groove on the front side and rood beam on the rear side. Eventually, a high accuracy sensor with maximum sensitivity and minimum nonlinearity has been achieved.

4.3 Dynamic performance

In the field of high accuracy measurement, besides the sensitivity and linearity, the mechanical stability is also of significant factor for micro-high sensitive pressure sensors. The mechanical stability is depended upon the first natural frequency (1st) of the membrane structure (Huang and Zhang 2014). To stabilize the membrane, normally a higher first natural frequency is often expected. This is because the structure of the sensor will be damaged due to the resonance effect when its natural frequency and measured signal are approximate (Jia and Seshia 2016). As shown in Fig. 9, the dynamic behavior analysis results show that a high first resonance frequency of 42.1 kHz is achieved for the proposed membrane with an increment of 32.8 and 12.3% compared with the C-type and BMQI structures, respectively; while for the CBM structure the first resonance frequencies almost equal with each other. The results mean that the proposed membrane is as good as the CBM structure and is better in comparison with the C-type and BMQI membranes in terms of stability.

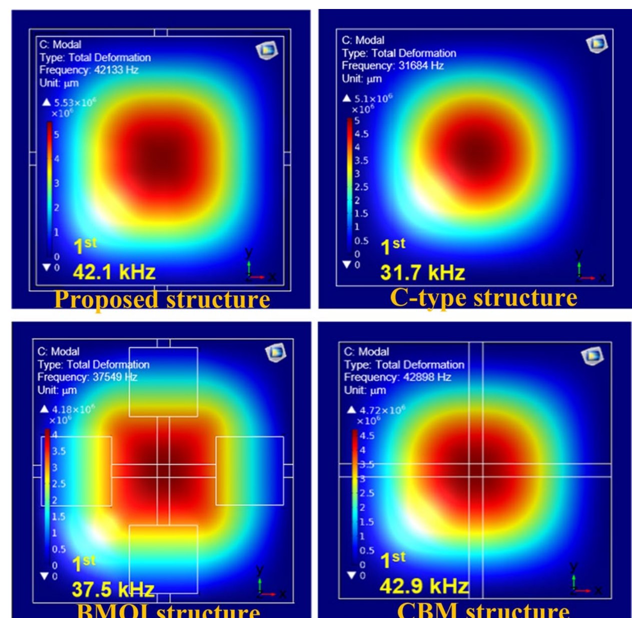

Fig. 9 Dynamic behavior of different membranes in the working range of 0–1 psi (6.895 kPa)

5 Conclusions

In this paper, it has been analyzed and compared the static and dynamic performance of different membrane structures for piezoresistive pressure sensors through FEM, including the C-, E-type, CBM, BMQI and proposed membranes. In comparison with CBM and BMQI structures, the proposed structure not only stiffened partially the membrane to reduce the nonlinearity and keep high first natural frequency, but also transferred more strain energy to the HCSP to guarantee even higher sensing sensitivity. Besides, the proposed membrane would minimize the size of the sensor chip while having same maximum stress than C- and E-type. Based on the simulation results, the proposed sensor achieved a high sensitivity of 34.5 mV/V/psi and a low nonlinearity of 0.25% FSS with the pressure range 0–1 psi. In terms of sensitivity, precision and linearization, these results suggested that the proposed structure had stable performance in micro-size, and it was a better choice for measuring micro-pressure in the field of biomedical applications.

Acknowledgements The work was supported by the China Scholarship Council for studying abroad (File No. 201508320275) and Erasmus+ project (2015-1-ES01-KA107-015460).

Compliance with ethical standards

Conflict of interest The authors declare that they have no conflict of interest.

References

Albert Chiou J, Chen S (2008) Pressure nonlinearity of micromachined piezoresistive pressure sensors with thin diaphragms under high residual stresses. Sens Actuators A Phys 147:332–339. doi:10.1016/j.sna.2008.03.012

Alpuim P, Correia V, Marins ES et al (2011) Piezoresistive silicon thin film sensor array for biomedical applications. Thin Solid Films 519:4574–4577. doi:10.1016/j.tsf.2011.01.300

Aryafar M, Hamedi M, Ganjeh MM (2015) A novel temperature compensated piezoresistive pressure sensor. Measurement 63:25–29. doi:10.1016/j.measurement.2014.11.032

Bao M (2005) Analysis and design principles of MEMS devices. Elsevier Science, Amsterdam

Bao M, Yu L, Wang Y (1991) Stress concentration structure with front beam for pressure sensor. Sens Actuators A Phys 28:105–112. doi:10.1016/0924-4247(91)85019-K

Dau VT, Tung BT, Dinh TX et al (2013) A micromirror with CNTs hinge fabricated by the integration of CNTs film into a MEMS actuator. J Micromech Microeng 23:75024. doi:10.1088/0960-1317/23/7/075024

Fraga MA, Furlan H, Massi M et al (2010) Fabrication and characterization of a SiC/SiO_2/Si piezoresistive pressure sensor. Procedia Eng 5:609–612. doi:10.1016/j.proeng.2010.09.183

Hao X, Maenaka K, Takao H, Higuchi K (2014) An analytical thermal-structural model of a gas-sealed capacitive pressure sensor with a mechanical temperature compensation structure. Sens Actuators A Phys 205:92–102. doi:10.1016/j.sna.2013.10.029

Herrera-May AL, Soto-Cruz BS, López-Huerta F, Aguilera Cortés LA (2009) Electromechanical analysis of a piezoresistive pressure microsensor for low-pressure biomedical applications. Rev Mex Fis 55:14–24. http://www.scielo.org.mx/pdf/rmf/v55n1/v55n1a3.pdf. Accessed 16 Jan 2017

Hsu T (2008) MEMS and microsystems: design, manufacture, and nanoscale engineering. Wiley, Hoboken

Huang X, Zhang D (2014) A high sensitivity and high linearity pressure sensor based on a peninsula-structured diaphragm for low-pressure ranges. Sens Actuators A Phys 216:176–189. doi:10.1016/j.sna.2014.05.031

Jia Y, Seshia AA (2016) Five topologies of cantilever-based MEMS piezoelectric vibration energy harvesters: a numerical and experimental comparison. Microsyst Technol 22:2841–2852. doi:10.1007/s00542-015-2599-z

Johnson RH, Karbassi S, Sridhar U, Speldrich B (1992) A high-sensitivity ribbed and bossed pressure transducer. Sens Actuators A Phys 35:93–99. doi:10.1016/0924-4247(92)80146-T

Kumar SS, Pant BD (2014) Design principles and considerations for the "ideal" silicon piezoresistive pressure sensor: a focused review. Microsyst Technol 20:1213–1247. doi:10.1007/s00542-014-2215-7

Kumar SS, Pant BD (2015) Polysilicon thin film piezoresistive pressure microsensor: design, fabrication and characterization. Microsyst Technol 21:1949–1958. doi:10.1007/s00542-014-2318-1

Kumar SS, Pant BD (2016) Effect of piezoresistor configuration on output characteristics of piezoresistive pressure sensor: an experimental study. Microsyst Technol 22:709–719. doi:10.1007/s00542-015-2451-5

Kumar SS, Ojha AK, Pant BD (2016) Experimental evaluation of sensitivity and non-linearity in polysilicon piezoresistive pressure sensors with different diaphragm sizes. Microsyst Technol 22:83–91. doi:10.1007/s00542-014-2369-3

Li S, Zhang Z, Tang J, Ding D (2014) A novel signal conditioning circuit for piezoresistive pressure sensor. Unifying Electr Eng Electron Eng 238:1707–1713. doi:10.1007/978-1-4614-4981-2_187

Li C, Cordovilla F, Jagdheesh R, Ocaña JL (2016) Design and optimization of a novel structural MEMS piezoresistive pressure sensor. Microsyst Technol. doi:10.1007/s00542-016-3187-6

Lin L, Chu H-C, Lu Y-W (1999) A simulation program for the sensitivity and linearity of piezoresistive pressure sensors. J Microelectromechanical Syst 8:514–522. doi:10.1109/84.809067

Marco S, Samitier J, Ruiz O et al (1996) High-performance piezoresistive pressure sensors for biomedical applications using very thin structured membranes. Meas Sci Technol 7:1195–1203. doi:10.1088/0957-0233/7/9/002

Meng X, Zhao Y (2016) The design and optimization of a highly sensitive and overload-resistant piezoresistive pressure sensor. Sensors (Basel) 16:348–359. doi:10.3390/s16030348

Mishra A, Bahal I, Arya J et al (2015) Sensitivity analysis of MEMS based piezoresistive sensor using COMSOL multiphysics. Adv Intell Syst Comput 327:59–67. doi:10.1007/978-3-319-11933-5_8

Park J, Kim J-K, Patil SJ et al (2016) A wireless pressure sensor integrated with a biodegradable polymer stent for biomedical applications. Sensors (Basel) 16:809–819. doi:10.3390/s16060809

Pramanik C, Saha H, Gangopadhyay U (2006) Design optimization of a high performance silicon MEMS piezoresistive pressure sensor for biomedical applications. J Micromech Microeng 16:2060–2066. doi:10.1088/0960-1317/16/10/019

Rajavelu M, Sivakumar D, Joseph Daniel R, Sumangala K (2014) Perforated diaphragms employed piezoresistive MEMS pressure sensor for sensitivity enhancement in gas flow measurement. Flow Meas Instrum 35:63–75. doi:10.1016/j.flowmeasinst.2013.12.004

Sharma A, Mukhiya R, Kumar SS, Pant BD (2013) Design and simulation of bulk micromachined accelerometer for avionics application. VLSI Des Test 382:94–99. doi:10.1007/978-3-642-42024-5_12

Song JW, Lee J-S, An J-E, Park CG (2015) Design of a MEMS piezoresistive differential pressure sensor with small thermal hysteresis for air data modules. Rev Sci Instrum 86:65003. doi:10.1063/1.4921862

Tian B, Zhao Y, Jiang Z (2010) The novel structural design for pressure sensors. Sens Rev 30:305–313. doi:10.1108/02602281011072189

Tian B, Zhao Y, Jiang Z, Hu B (2012) The design and analysis of beam-membrane structure sensors for micro-pressure measurement. Rev Sci Instrum 83:45003. doi:10.1063/1.3702809

Timoshenko S, Woinowsky-Krieger S (1959) Theory of plates and shells. McGraw-Hill Kogakusha, Tokyo

Ugural AC (1981) Stresses in Plates and Shells. McGraw-Hill, New York

Wang L, Li J (2014) A piezoresistive flounder element based on conductive polymer composite. Sens Actuators A Phys 216:214–222. doi:10.1016/j.sna.2014.05.010

Yao Z, Liang T, Jia P et al (2016) A high-temperature piezoresistive pressure sensor with an integrated signal-conditioning circuit. Sensors 16:913–925. doi:10.3390/s16060913

Yasukawa A, Shimazoe M, Matsuoka Y (1989) Simulation of circular silicon pressure sensors with a center boss for very low pressure measurement. IEEE Trans Electron Devices 36:1295–1302. doi:10.1109/16.30935

Yu H, Huang J (2015) Design and application of a high sensitivity piezoresistive pressure sensor for low pressure conditions. Sensors (Basel) 15:22692–22704. doi:10.3390/s150922692

Yu Z, Zhao Y, Sun L et al (2013) Incorporation of beams into bossed diaphragm for a high sensitivity and overload micro pressure sensor. Rev Sci Instrum 84:15004. doi:10.1063/1.4775603

Yu Z, Zhao Y, Li L et al (2015) Realization of a micro pressure sensor with high sensitivity and overload by introducing beams and Islands. Microsyst Technol 21:739–747. doi:10.1007/s00542-014-2234-4

Zhang S, Wang T, Lou L et al (2014a) Annularly grooved diaphragm pressure sensor with embedded silicon nanowires for low pressure application. J Microelectromechanical Syst 23:1396–1407. doi:10.1109/JMEMS.2014.2313635

Zhang X, Wang E, Yang X (2014b) Design and simulation of Nano-diamond film pressure sensor. Vacuum 99:189–191. doi:10.1016/j.vacuum.2013.05.023

Zhang J, Zhao Y, Ge Y et al (2016) Design optimization and fabrication of high-sensitivity soi pressure sensors with high signal-to-noise ratios based on silicon nanowire piezoresistors. Micromachines 7:187. doi:10.3390/mi7100187